Visions and Strategies for Reinforcing Additively Manufactured Constructions 2025

Contribution to the symposium

https://doi.org/10.52825/ocp.v7i.2771

Published: 12 Dec. 2025

Encasement of Pre-Placed Reinforcement in Injection 3D Concrete Printing: the Effect of Rheology and Process Parameters

Ando Jacobi[1,*], Jan-Philipp Zöllner[2], Norman Hack[2], and Inka Mai[1]

[1]Institute of Civil Engineering, Technische Universität Berlin

[2]Institute of Structural Design, Technische Universität Braunschweig

*Correspondence: Ando Jacobi, a.jacobi@tu-berlin.de

Abstract. Injection 3D Concrete Printing (I3DCP) is a new additive manufacturing technique, where material is robotically injected into a carrier liquid where it remains suspended. The injection of concrete into a non-hardening carrier liquid, has proven to be successful at producing complex and filigree concrete structures. I3DCP is capable of overcoming the directional limitations faced by other additive fabrication methods as it is possible to print in 3-dimensional space. However, this technology has been limited to producing compression-only structures, as its thin concrete strands are incapable of withstanding significant tensile loads. A potential solution is the introduction of reinforcement into the concrete structures. This study focuses on the injection of a fine grain concrete into well-characterized carrier liquids where spatially fixed rebars are placed to be fully encased. The effect of material- and process related parameters on the encasement quality are studied. The rheological parameters of the carrier liquid are varied by solid volume fraction (ranging from 33.3 vol.-% to 44.4 vol.-%). The shape of the nozzle (straight tube/ U-slot) and the nozzle traverse speed (ranging from 40 mm/s to 100 mm/s) are systematically studied as part of the process parameters. The quality of the encasement is evaluated by image analysis. It is observed that with increasing yield stress of the carrier liquid the reinforcement is less encapsulated while carrier liquids with a low yield stress are incapable of supporting the injected concrete. These effects can be counteracted by changing the nozzle shape and/or print speed. Finally, the potential and limitations of using reinforcement bars in I3DCP are discussed.

Keywords: Injection 3D Concrete Printing, Rebar Integration, Material-Process-Interaction, Additive Manufacturing in Construction

1. Introduction and Motivation

During Injection 3D Concrete Printing (I3DCP) either concrete or suspension is injected into a suspending medium which can be either hardening or non-hardening. Three material combinations are conceptually viable [1]: Concrete in Suspension (CiS), Concrete in Concrete (CiC) and Suspension in Concrete (SiC). This study focuses on the CiS variant in I3DCP during which concrete is injected into a non-hardening carrier liquid and remains stable in the suspension until it has hardened sufficiently to be removed from the carrier liquid. In order to support the injected concrete, mainly the density and yield stress of the carrier liquid are of importance [2]. The concrete is robotically injected into the carrier liquid using a cylindrical nozzle in form of a steel tube. This method allows for the fabrication of complex structures with comparatively few directional limitations as the carrier liquid is providing a support structure. The

resulting geometries typically consist of many individual strands of concrete which are connected at nodes (see *Figure 1*). The size of the strands is determined by the nozzle size, the concrete volume flow and the nozzle traverse speed of the robot. The shape of the strand may be circular or distorted (drop-shape, irregular ellipsoidal) as well as straight, discontinuous or undulating and is mainly determined by the relation of the nozzle speed and geometry as well as the concrete volume flow and the rheological properties of the carrier liquid [2]. Moreover, the rheological properties of the injected material might be of importance.

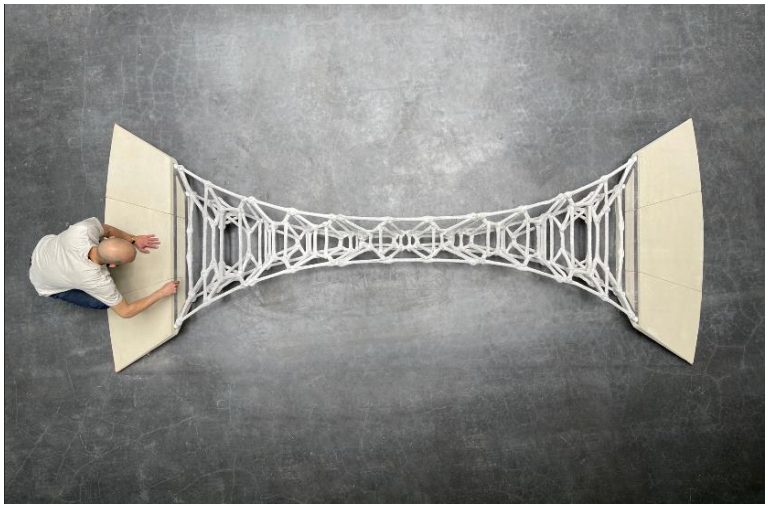

Figure 1. *Top view of a 3-metre-span bridge consisting of 5 pieces printed with I3DCP which was fabricated at TU Braunschweig*

Since one of the major advantages of I3DCP is the low amount of material used, the fabricated strands tend to be comparatively thin. Therefore, one significant limitation of I3DCP structures is the fragility of the individual concrete strands. Without reinforcement these are incapable of withstanding significant tensile loads. This is highlighted by the fact that thus far I3DCP structures are designed to primarily result in compressive loads [3]. This limitation could be overcome by introducing reinforcement into I3DCP. However, up to now there is no systematic investigation on reinforcement integration in I3DCP. Lowke et al. have explored the concept of printing around pre-installed steel reinforcement bars in I3DCP [2]. Utilizing reinforcement bars has the advantage that it is a cost-effective method and the material is widely available. The aim in [2] was to encase pre-installed reinforcement bars during the printing process. Their results showed that an encasement of the reinforcement is viable, however a slight seam was found where concrete did not encase the reinforcement. They point out that process and material parameters are likely to affect the encasement quality of the reinforcement. Therefore, this study aims at further exploring the introduction of reinforcement bars into I3DCP by systematically investigating the effect of relevant material and process parameters. In this study carrier liquids with varying solid volume fractions, i.e. varying yield stresses, are tested. Additionally, the effect of the nozzle traverse speed and the nozzle geometry are investigated as process parameters.

2. Materials and Methods

2.1 Experimental Matrix

The following settings are investigated:

- the nozzle traverse speed with 40/60/80 and 100 mm/s,
- the solid-volume fraction of the carrier liquid ranging from 33.3/37.5/41.2 to 44.4 vol.-% and
- the geometry of the nozzle-tip with a Straight Tube (ST) and U-Slot (US) nozzle.

In total four different carrier liquids are used (see *Table 1*). In each carrier liquid four different nozzle traverse speeds are tested. The two different nozzle tips are both tested in all carrier liquid and nozzle traverse speed settings, leading to 32 experimental settings in total with one repetition per setting.

2.2 Injected material and carrier liquid

As injected material for encasing reinforcement a fine grain concrete is used, which is composed of cement CEM I 42.5R, limestone powder, sand with a maximum grain size of 0.5 mm, water, superplasticizer and cellulose ether. The water/cement-ratio is 0.42 and the volumetric sand to paste ratio is 0.56. The mix exhibits with a yield stress of 52.5 Pa – compared to other printing techniques – a high workability and eases pumpability. Carrier Liquids (CL) with varying solid volume fractions between 33.3 vol.-% and 44.4 vol.-% are used. The CLs primary ingredients are water and limestone powder which are mixed to create an aqueous liquid. Moreover, the CL also contains cellulose ether as it improves the stability of the mixture throughout the testing. The mixture composition of the CLs and its yield stress is given in *Table 1*. For reinforcement 8 mm rebars with a length of approximately 560 mm – matching the length of the container – are used.

Table 1. *Carrier Liquid (CL) mixtures with varying solid volume fractions and thereby yield stresses*

CL Name	Solid Volume Fraction (vol.-%)	cellulose ether	Yield Stress (Pa)
CL33.3%	33.3	0.5% bwow	7.2
CL37.5%	37.5	0.5% bwow	16.1
CL41.2%	41.2	0.5% bwow	32.5
CL44.4%	44.4	0.5% bwow	59.9

2.3 Printing Setup

For each printing procedure, four reinforcement bars are fixed inside a container, raised 120 mm above the bottom. The rebars are spaced 90 mm apart and the outer rebars are distanced 45 mm from the walls of the container. At least 400 mm of each rebar is exposed for encasement by means of I3DCP (see *Figure 2*).

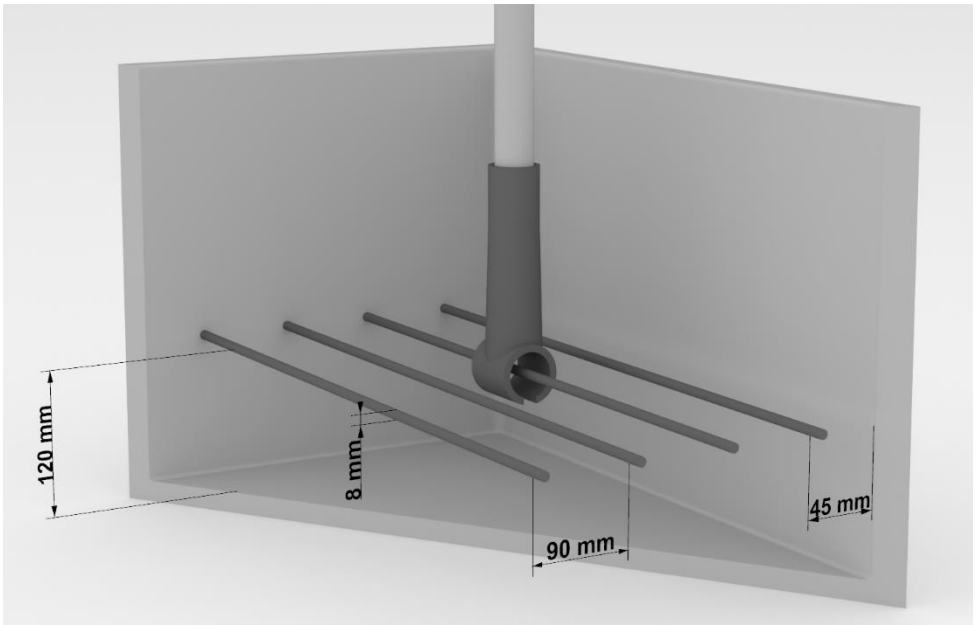

Figure 2. *Visualization of the printing process using the US nozzle.*

Two different nozzles are used in this study. The first nozzle is a pipe with an inner diameter of 30 mm and a wall thickness of 2 mm, i.e., outer diameter of 34 mm (see *Figure 3*). This nozzle is from now on referred to as the Straight Tube (ST). The second nozzle was modified with the intention to guide the concrete around the rebar during the injection process. It can be attached to the ST nozzle but then transitions into an orthogonal U-shaped arc with a radius of 19 mm. At the very bottom there is a gap with a width of 12 mm to allow the rebar to pass through. This nozzle is referred to as the U-Slot nozzle (US).

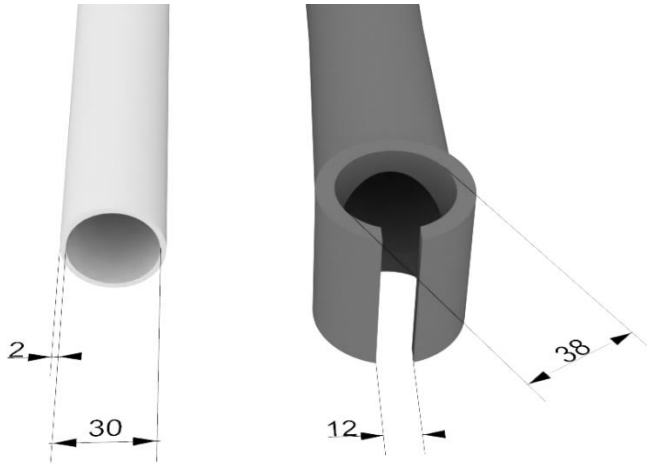

Figure 3. *Visualisation of different nozzle geometries, the ST nozzle (left) and the US nozzle (right)*

After the rebars are fixed in the empty containers the robot path for each individual rebar is calibrated. During the entire printing process, the nozzle remains in a vertical orientation. When using the ST nozzle, it is centred 5 mm above the rebar. The US nozzle is calibrated so the rebar is in the focal point of the arc. After successful calibration the carrier liquid is filled into the container until 60 mm above the rebar.

In order to pump the concrete a MAI®2PUMP PICTOR-3D is utilized with a constant concrete volume flowrate of 5.1 L/min. The nozzle is moved using a UR10e robot by Universal Robots.

2.4 Evaluation Methods for Encasement Quality

The specimens are tested with regard to the successful encasement of reinforcements in concrete using two methods: a) the weighing of the connected concrete and b) the visual inspection of the cross section via image analysis. The encasement quality is chosen as the main relevant parameter as it has proven in [4] that the encasement governs the mechanical bonding between reinforcement and concrete. Moreover, it is a crucial parameter for the durability of a structure.

2.4.1 Weight of attached concrete

The weight of concrete remaining attached to the reinforcement can be used as a simple indicator for printing failure. For the printed length of 400 mm any concrete weight below 19.8 g/cm, i.e. on average less than 15 mm of concrete cover, were deposited around the rebar when assuming an ideal distribution of concrete. This can be considered insufficient as concrete cover for reinforcement protection [5]. The concrete weight only serves as an indicator for failure, but not for success as it lacks consideration of the concrete distribution around the reinforcement which is important for successful encasement. Therefore, this investigation serves as a pre-selection criterion for further visual inspection.

2.4.2 Visual inspection of the cross section

The specimen which are encased by a sufficient amount of concrete are cut perpendicular to the reinforcement bar in order to inspect their cross-section by image-analysis (see *Figure 4 a)*). Each specimen is cut 5 times and the results are averaged. The cross section is analysed, by scanning it and then allocating each pixel to one of three areas: i) the reinforcement, ii) the concrete and iii) voids in the concrete which can be filled by both, air or limestone (see exemplary distorted cross section in *Figure 4 b)* which exhibits all three areas). For the allocation of the pixels a Multi-Layer Perceptron Classifier (MLPClassifier) is used [6]. For each pixel type a MLPClassifier was trained to identify the respective type by looking at the red, green and blue colour values of a 5 px by 5 px square with the pixel in question at its centre. The training data was produced by manually separating areas from five cross section images. All automatically segmented images were manually controlled after segmentation. Three measures of encasement quality are derived from this:

1. the encasement rate in the direct proximity to the reinforcement (within 2mm from the rebar surface), which is defined as the percentage of the total considered area filled by concrete. This measure can be used to judge the quality of the connection between the reinforcement bar and the concrete,
2. the encasement rate within 15 mm of the reinforcement, which is often used as the recommended concrete covering to shield the reinforcement from corrosion and other outside influences and to ensure the safe transmission of bond forces [5],
3. the overall uniformity of the cross section given by the standard deviation of the distance between the reinforcement and the surface of the specimen. Here the distance is determined in 100 evenly spaced directions with the rebar at the centre. This measure considers both the sphericity of the cross section and the centeredness of the reinforcement. A higher standard deviation is caused by a more distorted strand or an ill positioning of the reinforcement.

These measures are highlighted in *Figure 4 c)*.

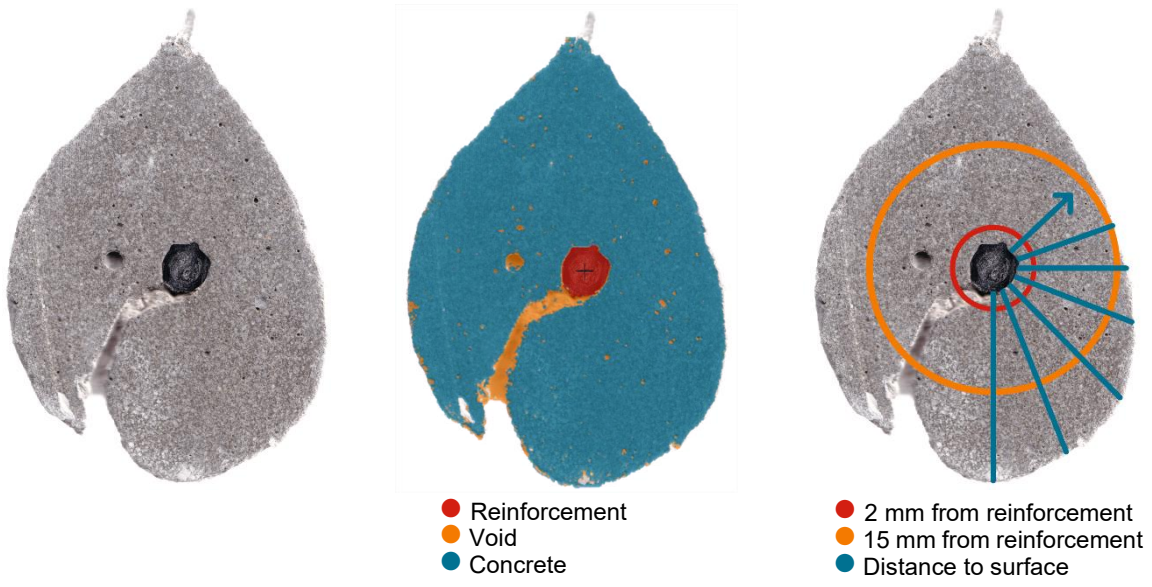

a) *Scan of cross section*

b) *Scan of cross section with different areas highlighted*

c) *Scan of cross section with measures of quality visualized*

Figure 4. *Scan of a distorted cross section of specimen manufactured using the US nozzle, CL41.7% and a nozzle traverse speed of 40 mm/s revealing reinforcement, voids and concrete. The reinforcement has an average diameter of 8 mm.*

The cutting of the specimens can cause the reinforcement bar to fall out of the concrete if it has not connected well enough. In that case the image analysis is performed with reference to the reinforcements original position, since the analysis can still prove useful for contextualizing other results. *Table 2* gives the number of cuts where the reinforcement remained in its original position for each setting.

Table 2. *Number of cross sections where the reinforcement bar remained connected to the concrete after cutting*

	Nozzle / Carrier liquid			
	ST		**US**	
Traverse speed	**CL41.2%**	**CL44.4%**	**CL41.2%**	**CL44.4%**
40 mm/s	5	3	5	5
60 mm/s	5	1	5	4
80 mm/s	5	3	3	1
100 mm/s	3	5	0	0

3. Results

3.1 Pre-selection for in depth investigation via weighing

The fabricated specimens were first assessed by their respective concrete weight, the results of which are given in *Table 3* and *Table 4* for the ST and US nozzle respectively. For the ST nozzle the attached concrete to the rebar varies between approx. 0.28 g/cm for CL 33.3% up to 67 g/cm for CL 41.2%. It can be observed that with an increase in solid volume fraction of the carrier liquid there is an increase in attached amount concrete to the rebar. Moreover, it is observed that the amount of material decreases with an increase in traverse speed. This is an expected outcome as the concrete volume flow is not changed and the traverse speed is herewith linked directly to the amount of applied concrete per running meter of rebar. From this the attachment rate, meaning the percentage of injected concrete which attached to the reinforcement, can be determined by considering the concrete flow rate, the nozzle traverse speed, the length of the nozzle path and the density of the concrete in fresh state. In CL33.3% and CL37.5% when using the ST nozzle only between 1% to 12% of the injected concrete actually stayed attached to the reinforcement. When using the US nozzle these numbers increased to a 2% to 33% attachment rate. While the results for both nozzles remain well below the desired 100% of attachment rate for CL33.3% and CL37.5%, the usage of the US nozzle clearly has a positive effect on the amount of attached concrete. This is even more pronounced for higher nozzle traverse speeds. For CL41.2% and CL44.4% at least 100% of concrete attached to the rebar. An attachment rate above 100% can be explained by additional concrete that was deposited during the vertical approach and departure of the nozzle to and from the rebar.

Table 3. *Concrete weights per cm and % of injected concrete for specimens produced using the ST nozzle*

Traverse speed (mm/s)	**CL33.3%**		**CL37.5%**		**CL41.2%**		**CL44.4%**	
	g/cm	**%**	**g/cm**	**%**	**g/cm**	**%**	**g/cm**	**%**
40	0.30	1	2.38	4	67.00	117	61.25	107
60	0.28	1	2.4 0	6	38.38	100	46.03	120
80	0.28	1	1.95	7	26.05	91	37.00	129
100	0.30	1	2.70	12	21.28	93	24.60	107

Table 4. *Concrete weights per cm and % of injected concrete for specimens produced using the US nozzle*

Traverse speed (mm/s)	**CL33.3%**		**CL37.5%**		**CL41.2%**		**CL44.4%**	
	g/cm	**%**	**g/cm**	**%**	**g/cm**	**%**	**g/cm**	**%**
40	0.95	2	1.70	3	62.23	109	60.50	105
60	0.68	2	3.35	9	47.93	125	48.98	128
80	1.43	5	4.50	16	39.65	138	39.25	137
100	3.30	14	7.68	33	25.43	111	36.6 ^{0}	160

Only the cross sections of the specimens fabricated using CL41.2% and CL44.4% were subsequently cut and inspected using image analysis as the other specimens were not encased by at least 19.8 g/cm of concrete, which is assumed to be the minimal amount of concrete needed to ensure sufficient concrete cover of 15 mm.

3.2 Encasement Quality

In *Figure 6* the results from the image analysis on encasement quality are shown and will be further discussed in the following subsection 4.2.1 to 4.2.3. In *Figure 6 a)* and *b)* the encasement rate for various traverse speeds, nozzle types and carrier liquids is shown for the 2 mm radius and 15 mm radius from the surface of the rebar respectively. The average encasement rates within 2 mm of the surface of the reinforcement bar range from 34.8% to 75.6%. For the average encasement rates within 15 mm from the rebar these numbers increase to the range between 46% and 93.3%. Many specimens exhibit voids filled with carrier liquid directly at the reinforcement, which can be seen in *Figure 5 a)*. These pockets likely cause the lower average encasement rate for the 2 mm radius compared to the 15 mm radius since they account for a greater percentage of the total area at a smaller radius. For some specimen the reinforcement remains partially exposed leading to a significantly lower encasement rate, see *Figure 5 b)*. The cross-section shown in *Figure 5 a)* has a comparatively good encasement quality with a 2 mm encasement rate of 85%, a 15 mm encasement rate of 96% and a standard deviation of

a) *Cross-section within 15 mm of the reinforcement with an encasement rate of 85% within a 2 mm radius*

b) *Cross-section within 15 mm of the reinforcement with an encasement rate of 51% within a 2 mm radius*

Figure 5. *Exemplary specimens printed in CL41.2% using the ST nozzle, with a) exhibiting a high encasement rate for a nozzle traverse speed of 40 mm/s and b) exhibiting a low encasement rate for a nozzle traverse speed of 100 mm/s*

8.2 mm. In contrast the cross-section shown in *Figure 5 b)* has a poorer encasement quality with a 2 mm encasement rate of 51%, a 15 mm encasement rate of 77% and standard deviation of 8.5 mm. As is shown in *Figure 6 c)* the average standard deviation of the distance from the reinforcement to the surface of the specimen varies for the different settings between 4.5 mm and 15 mm. Notably the usage of the US nozzle often results in a more uniform distribution of the concrete around the reinforcement bar.

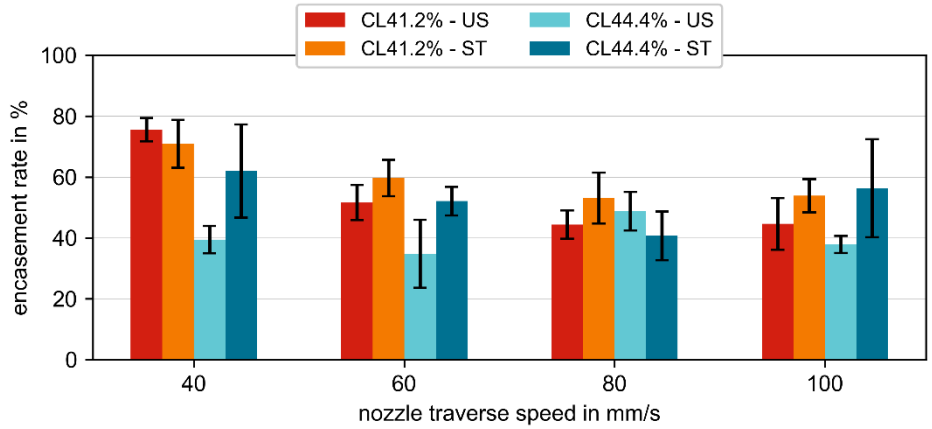

***a)** average encasement rate within 2 mm of the reinforcement bar with standard deviation*

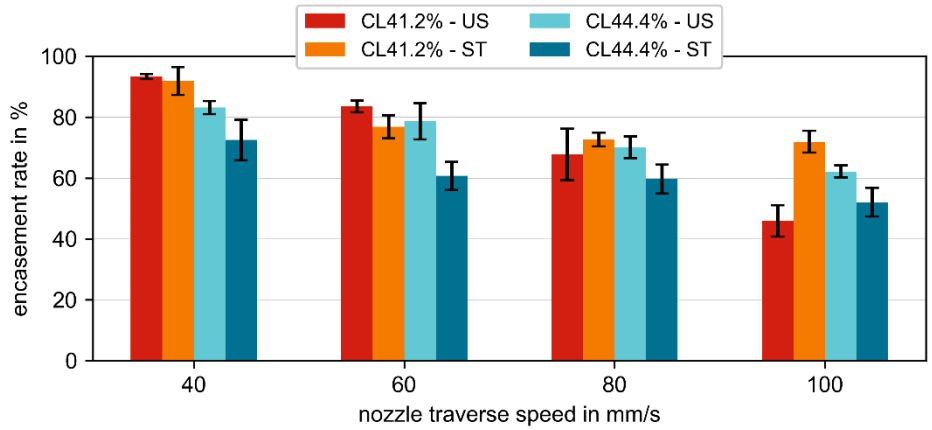

***b)** average encasement rate within 15 mm of the reinforcement bar with standard deviation*

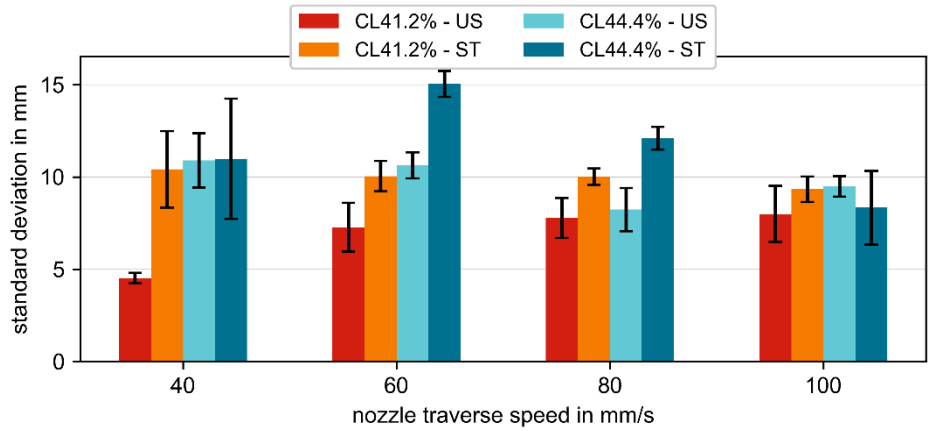

***c)** average standard deviation of the distance from the reinforcement to the surface of the specimen with standard deviation*

***Figure 6.** Image analysis of cross sections for different nozzle traverse speeds*

3.2.1 Effect of Carrier Liquid's Yield Stress

The solid volume fraction of the carrier liquid and herewith the yield stress significantly influences the results of the tests. This is particularly apparent in *Figure 6* a) and b), particularly for lower nozzle traverse speeds where the usage of CL41.2% (red and orange bars) and thereby lower yield stress results in higher encasement rates and better sphericity than the usage of CL44.4% (dark and light blue bars). Although a lower yield stress of the carrier liquid seems to be beneficial, the yield stress should not be too low, as the lower solid volume fractions appear

to be unable to support the concrete causing strands to sink to the bottom of the containers, as for CL33.3% and CL37.5%, see *Table 3* and *Table 4*. When injected into CL41.2% and CL44.4% the concrete remained in suspension and did not sink. In

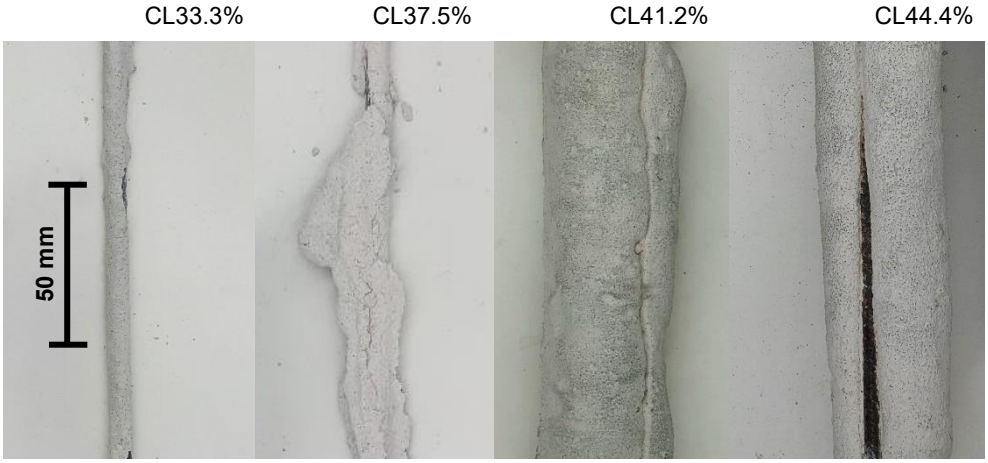

Figure **7** this effect can be observed exemplary as in CL33.3% barely any concrete attached to the rebar, in CL37.5% some concrete remained attached and in CL41.2% and CL44.4% significant amounts of concrete encased the rebar. It is assumed that the yield stress of CL33.3% and CL37.5% is not high enough to sustain the forces generated by the injected material, which causes it to sink to the bottom of the container. However, CL41.2% and CL44.4% have a sufficiently high yield stress and herewith material remains suspended and attached to the rebar.

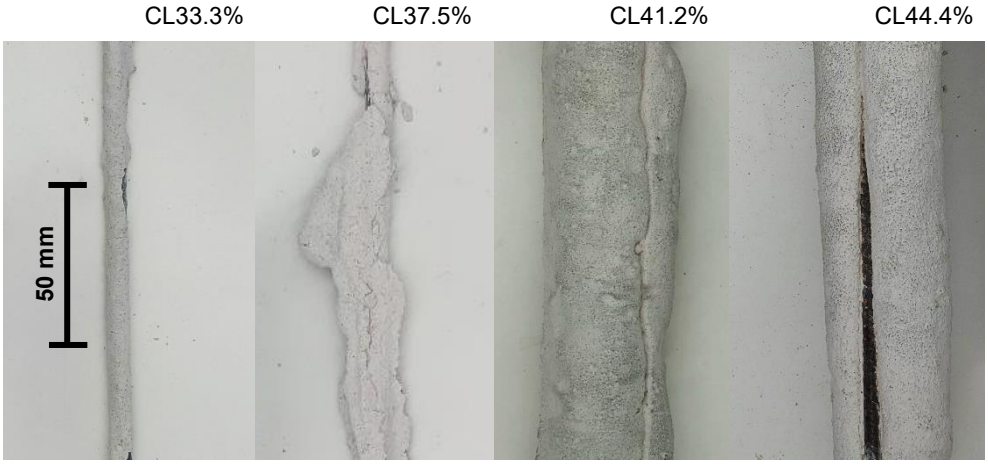

Figure 7. *Four specimens fabricated using varying carrier liquids with increasing solid volume fraction, the ST nozzle and a nozzle traverse speed of 40 mm/s. The two leftmost specimens were not cut and further analysed as they lack sufficient concrete covering.*

The image-analysis of the cross sections of the specimens produced in CL41.2% and CL44.4% shows that a lower solid volume fraction, i.e., lower yield stress, correlates with better encasement both within 2 mm and 15 mm radius around the rebar, see *Figure 6 a)* and *b)*. For example, when using the ST nozzle and a traverse speed of 40 mm/s, CL41.2% corresponds to an average encasement rate of approx. 70% whereas CL 44.4% corresponds to approx. 60%, compare orange and dark blue bars in *Figure 6 a)*. This trend is especially distinct for lower traverse speeds of the nozzle. Similarly, a lower standard deviation of the distance from reinforcement to surface and thereby a better uniformity of the shape of the strand around the reinforcement was observed for CL41.2%. It is suspected that the lower yield stress and viscosity allow for an easier flow around the rebar. Conversely, a higher yield stress is suspected

to hinder a full encasement as it prevents the concrete from fully flowing around the reinforcement.

These observations are also highly dependent on the nozzle geometry. When using the ST nozzle, a reduction of the yield stress consistently leads to an improved encasement. The same holds true for the US nozzle at low nozzle traverse speeds, however at higher speeds this trend is reversed. These effects become apparent in *Figure 8 a)* where CL41.2% shows a better 15 mm encasement rate for the ST nozzle and *Figure 8 b)* where the results for the US nozzle in CL41.2% diverge to a greater extent. The difference at low nozzle traverse speeds is more pronounced when considering the 2 mm encasement rate than the 15 mm encasement rate. This difference between the 2 mm encasement rate and the 15 mm encasement rate could be explained by voids directly under the reinforcement – visible in *Figure 5 a)* – which are present in many specimens and have a higher impact on the 2 mm encasement rate. It is likely that the larger cross-section of the US nozzle can have an adverse effect on the encasement quality which plays a greater role in carrier liquids with a higher viscosity and at higher speeds, see *Figure 8 b)*.

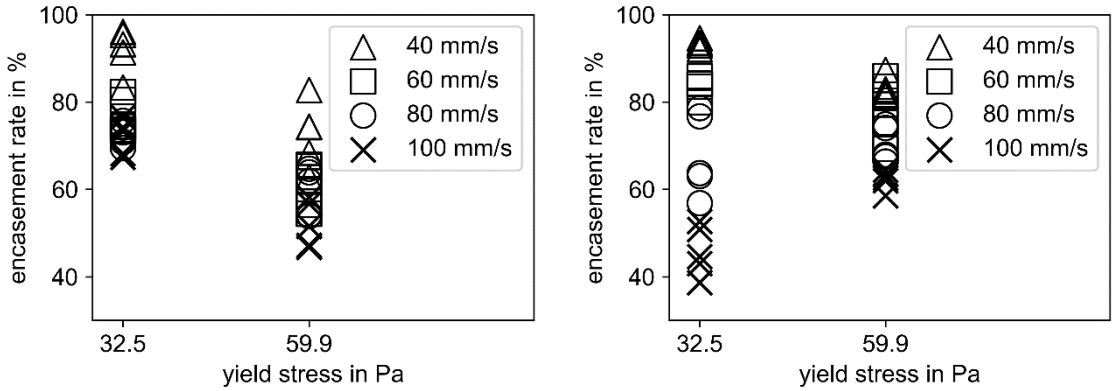

Figure 8. *Encasement rate within 15 mm of the reinforcement surface for a) the ST nozzle and b) the US nozzle.*

3.2.2 Effect of Nozzle Traverse Speed

With a higher nozzle traverse speed, a decrease in amount of attached concrete to the rebar is observed for CL41.2% and CL44.4%, see examples in *Figure 9*. This is an expected result, as the volume flowrate of the pump was kept constant throughout the tests. Hence a lower nozzle traverse speed results in less injected concrete as long as the concrete remains in suspension, see also *Table 3* and *Table 4* in the pre-study. Therefore, a better encasement of the rebar for lower traverse speeds can be observed, as can be seen in *Figure 9* and *Figure 6 a)* and *b)*. The uniformity of the specimens printed in CL41.2 with the ST nozzle and in CL44.4% with the US nozzle does not change significantly for different nozzle traverse speeds. However for those printed in CL41.2% with the US nozzle, lower nozzle traverse speeds correlate with a lower standard deviation of their radii and thereby an improved uniformity, see *Figure 6 c)*. This might be due to the combination of using the US nozzle and injecting into a carrier liquid with a lower yield stress taking better advantage of the additional concrete present at lower nozzle traverse speeds as it is guided around the rebar. These observations could not be made for CL33.3% and CL37.5% as these carrier liquids were unable of supporting the injected concrete. Overall lower nozzle traverse speeds appear to positively impact the encasement quality especially when using the US nozzle and a carrier liquid with a lower yield stress as these achieved by far the best uniformity. When printing at high nozzle traverse speeds it likely is beneficial to utilize the ST nozzle regardless of the carrier liquid.

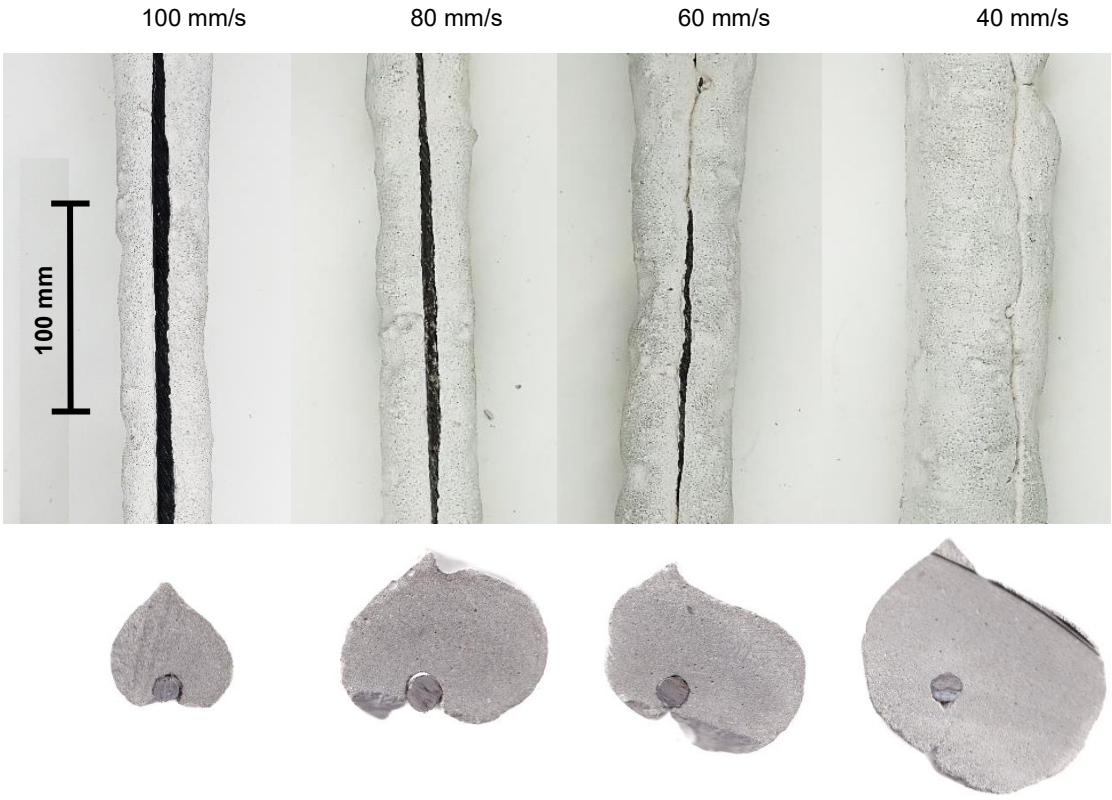

Figure 9. *Top view and distorted cross-sections of four specimens printed in CL41.2% using a ST nozzle with the nozzle traverse speeds 100 mm/s, 80 mm/s, 60 mm/s and 40 mm/s (left to right) exhibiting an increasing quality of encasement.*

3.2.3 Effect of Nozzle Geometry

For specimens fabricated using the US nozzle a lower nozzle traverse speed positively affects both, the 15 mm encasement rate and the uniformity of specimens compared to higher traverse speeds (see *Figure 6 b)* and *c)*). This effect is especially pronounced in CL41.2% where the specimens fabricated using the US nozzle exhibit a continuously improving encasement quality with reducing nozzle traverse speeds. For example, the 15 mm encasement rate of these specimens improves from 45% at a speed of 100 mm/s to 93% at a speed of 40 mm/s, as is shown in *Figure 6 b).* The results are less uniform for the ST nozzle where the encasement appears to improve with lower nozzle traverse speeds but the uniformity does not clearly correlate with the nozzle traverse speed. When visually inspecting the geometry of the cross sections of the printed strands a difference in shape becomes apparent (see *Figure 10*). The usage of the ST nozzle results in the concrete being mostly deposited on top of the reinforcement bar where the concrete forms into a drop shape. The US nozzle successfully guides the concrete around the reinforcement more evenly. The resulting geometry is more circular with the exception of the tip where a small edge remains and a notable seam at the bottom where the concrete did not fully encapsulate the reinforcement. It is generally observed that the size of this seam is inversely proportionate to the amount of concrete deposited which is effectively varied by the nozzle traverse speed. This observation is reflected in *Figure 6 c)* where the usage of the US nozzle seems to be mostly beneficial with regards to the sphericity and centeredness of the reinforcement, especially in CL41.2%.

a) *ST nozzle* ***b)*** *US nozzle*

Figure 10. *Cross section of two specimen fabricated using different nozzle geometries. Both were printed using CL44.4% and a nozzle traverse speed of 60 mm/s and resulted only in a partial encasement, leaving one side of the reinforcement exposed.*

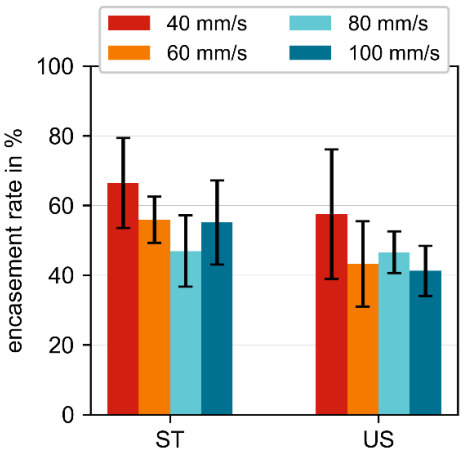

a) *average encasement rate within 2 mm of the reinforcement bar*

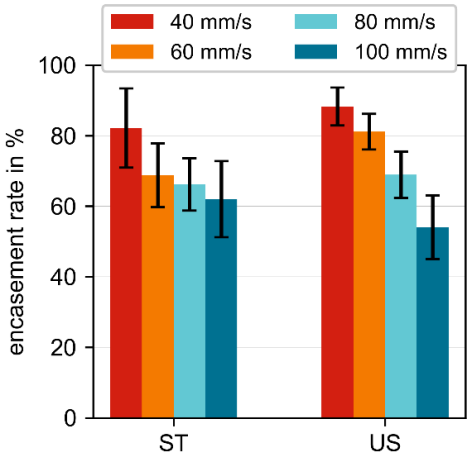

b) *average encasement rate within 15 mm of the reinforcement bar*

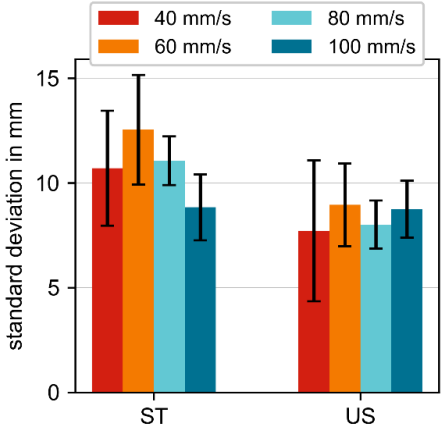

c) *average standard deviation of the distance from the reinforcement to the surface of the specimen*

Figure 11. *Image analysis of the cross sections for different nozzle geometries*

This effect, the improved sphericity and centeredness when using the US nozzle, is reflected in the difference of uniformity for the two nozzles shown in *Figure 11 c)* where on average the usage of the US nozzle decreases the standard deviation. *Figure 11* shows the results of the cross-section image analysis for the two different nozzle geometries. Here the results for the different carrier liquids were averaged. *Figure 11 a)* shows that the usage of the US nozzle leads to a slight decrease in the encasement rate within 2 mm of the rebar, in *Figure 11 b)* a mostly positive effect can be observed.

4. Discussion

All three of the tested parameters, the rheology of the carrier liquid, the nozzle traverse speed and the geometry of the nozzle significantly affect the geometry of the resulting specimens. The lack of stability when printing with CL33.3% and CL37.5% is likely caused by a significant difference in density between the carrier liquids and the concrete as well as their lower yield stresses. A higher solid volume fraction and thereby a higher density and yield stress enables the printing stability for I3DCP. The results of the visual inspection of the cross section suggest that a lower solid volume fraction of the carrier liquid increases the relative amount of concrete around the reinforcement bar. This likely results from an easier displacement of the carrier liquid by the concrete.

Many of the printed specimens exhibit a distorted cross section with an edge pointing upwards, as is visible in *Figure 10* and *Figure 12 b)*. This phenomenon has been described in [2] as being a result of dynamic cavities behind the moving nozzle. According to their assumptions the distorted geometry can be counteracted by reducing the nozzle traverse speed, the nozzle diameter, the viscous stresses resisting the flow and increasing the hydrostatic pressure by printing at a greater depth. The effect of some of these parameters was observed in this study and found to agree with the assumptions. Specimens printed with the US nozzle exhibit a more pronounced edge facing upwards, likely due to its larger cross section. The same is true for specimen printed in CL44.4% as its higher solid volume fraction results in greater viscous stresses. The nozzle traverse speed was varied but the resulting change in deposited concrete had a much more significant influence on the overall shape and therefore no conclusion can be drawn. The effect of the printing depth was not investigated and would need to be considered in future research. It is likely that the rheological properties of the injected concrete also play a significant role when it comes to encasement rate and shape of the strand. The concrete that was used here has a comparatively low viscosity which could worsen distortions as the concrete is more easily affected by the dynamic cavities.

a) *cross section of specimen fabricated using a ST nozzle in CL41.2% with a nozzle traverse speed of 40 mm/s*

b) *cross section of specimen fabricated using a US nozzle in CL44.4% with a nozzle traverse speed of 100 mm/s*

Figure 12. *example of two cross sections exhibiting successful and poor encasement quality*

On average lower nozzle traverse speeds achieve a better encasement quality as exemplified in *Figure 12 a)*. As a constant volume flow of mortar is injected, a lower nozzle traverse speed results in a greater amount of concrete encasing the reinforcement bar which likely benefits the encasement quality. Additionally, since lower speeds are associated with less distortion that allows for more concrete to flow around the reinforcement.

The usage of the US nozzle has improved the encasement quality for printing in CL41.2% while showing adverse effects when printing with CL44.4% possibly due to the previously mentioned greater distortions in more viscous carrier liquids.

It should be noted that all investigated parameters seem to significantly affect each other. As mentioned in 4.2.1 the US nozzle has a different impact for different carrier liquids. Similarly higher nozzle traverse speeds have a positive effect in CL33.3% and CL37.5% and a negative effect in CL41.2% and CL44.4%.

5. Conclusion

This study investigated the role of the solid volume fraction of the carrier liquid, the nozzle traverse speed and the nozzle geometry on the encasement quality of pre-placed reinforcement bars when using I3DCP. The effect of these parameters was measured by considering the reinforcement rate both directly at the rebar and around it as well as the geometric uniformity of the cross section of the printed strands. The observations of this study lead to the conclusion that a carrier liquid which is used for I3DCP around pre-positioned reinforcement bars must have a yield stress just high enough to reliably hold the injected material. In our case the minimum yield stress capable of supporting the injected concrete was 32.5 Pa. As long as this condition is fulfilled the carrier liquid should have a minimal viscosity for optimal encasement.

The utilization of the US nozzle has proven to be effective at a low nozzle traverse speed. For the common ST nozzle low speeds are also mostly beneficial. However, the usage of the US nozzle could lead to a more significant distortion of the cross-section of the specimens which should be counteracted by other measures such as lower nozzle traverse speeds and a greater printing depth. Overall, the optimal results under the given conditions were achieved when printing with the US nozzle into CL41.2% at the minimal tested nozzle traverse speed of 40 mm/s. It is likely that lower speeds could produce better results.

6. Outlook

The reinforcement integration in I3DCP is still at an early stage of development, but it holds considerable promise for advancing the frontier of knowledge in the nearer future and bringing the technology to the next level of application.

For real applications, voids in the vicinity of the reinforcement need to be prevented. As this study shows that material- and process parameters are able to greatly improve the quality of encasement, a further understanding of material-process-parameters is aimed at. Next steps will incorporate an investigation of even lower nozzle traverse speeds and other nozzle geometries with the aim to reduce distortion. Additionally, the concrete flowrate could be adjusted proportionally to the nozzle traverse speed in order to ensure that sufficient material is deposited. Material wise the effect of carrier liquid, especially higher yield stress, and the injected material’s rheological properties will be in focus.

Technically as a next step the localization of rebar and its automated placement and detection will be envisaged. So far only horizontal rebars have been investigated; non-horizontal rebars will need to be investigated especially as the depth of printing is assumed to have an effect on strand geometry and also on encasement of rebars. Currently the placement of the

rebar and the calibration of the nozzle path in relation to the rebar is done manually. For the future robot assisted reinforcement placement as well as automatic rebar detection will be implemented in the digital workflow of rebar encasement.

In the medium-term, also the encasement of complex rebar geometries and connected rebar geometries will be in focus, as these will be of relevance for real-application such as bridges, *Figure 13*. Only when addressing the component scale, I3DCP can be transferred from laboratory research to industrial practice.

Figure 13. *Bridge Design developed at ITE/TU Braunschweig in collaboration with Ole Ohlebrock and Pierluigi D'Acunto*

Author contributions

Ando Jacobi: Conceptualization, Investigation, Methodology, Writing – original draft

Jan-Philipp Zöllner: Conceptualization, Investigation, Methodology

Norman Hack: Supervision, Methodology

Inka Mai: Supervision, Methodology, Writing – review & editing

Competing interests

The authors declare that they have no competing interests.

Funding

The research was funded by the Deutsche Forschungsgemeinschaft (DFG, German Research Foundation) – Projektnummer 414265976 – TRR 277. The authors gratefully acknowledge the support provided by the DFG.

Acknowledgement

The authors thank Holcim GmbH who contributed the cement (Pur 4 R CEM I 42,5 R) and SE Tylose GmbH & Co. KG who contributed the Methylcellulose (MH 100000 P6) used in this study.

References

[1] Hack, N., Mai, I., Brohmann, L., Ganter, S., Lowke, D., Kloft, H., (2020). Injection 3D Concrete Printing (I3DCP): Basic Principles and Case Studies. In Materials, vol. 13, March 2020, doi: https://doi.org/10.3390/ma13051093

[2] Lowke, D., Vandenberg, A., Pierre, A., Thomas, A., Kloft, H., Hack, N., (2021). Injection 3D concrete printing in a carrier liquid - Underlying physics and applications to lightweight space frame structures. Cement and Concrete Composites, vol. 124, November 2021, doi: https://doi.org/10.1016/j.cemconcomp.2021.104169.

[3] Xiao, Z., Hack, N., Kloft, H., Lowke, D., Mai, I., D'Acunto, P., (2025). Constraint-based form-finding of space trusses for Injection 3D Concrete Printing through Vector-based Graphic Statics. Additive Manufacturing, vol. 103, April 2025, doi: https://doi.org/10.1016/j.addma.2025.104751

[4] Freund, N., Mai, I., Lowke, D. (2020). Studying the Bond Properties of Vertical Integrated Short Reinforcement in the Shotcrete 3D Printing Process. Second RILEM International Conference on Concrete and Digital Fabrication. DC 2020. RILEM Bookseries, vol 28. Springer, Cham. https://doi.org/10.1007/978-3-030-49916-7_62

[5] DIN EN 1992-1-1:2011-01, Eurocode 2: Design of concrete structures - Part 1-1: General rules and rules for buildings;

[6] Pedregosa, F., Varoquaux, Gaël, Gramfort, A., Michel, V., Thirion, B., Grisel, O., Blondel, M., Prettenhofer, P., Weiss, R., Dubourg, V., Vanderplas, J., Passos, A., Cournapeau, D. (2011). Scikit-Learn: Machine Learning in Python. Journal of Machine Learning Research, vol. 12, pp. 2825-2830, October 2012